Mineralium Deposita (2000) 35: 2–20

ARTICLE

V. Hanuš · J. Vaněk · A. Špičák

Seismically active fracture zones and distribution of large accumulations of metals in the central part of Andean South America

Received: 6 November 1997 / Accepted: 20 April 1999

Abstract The analysis of the geometry of distribution of earthquake foci in the central part of Andean South America between 18° and 34°S made the delineation of several seismically active fracture zones in the continental wedge overlying the subducting Nazca plate possible. Correlation of their position with the distribution of hypogene accumulations of metals revealed that the majority of large mineral deposits and mining districts are situated in the outcrops of these fracture zones. We present geometrical documentation (map of epicentres, vertical and longitudinal cross sections) of the most important fracture zones and data on mineralogical composition, genetic type and available radiometric ages of mineral deposits. Sixteen mining districts in Chile, and 24 in Argentina, were attributed to the seismically active fracture zones. Major mining districts and individual large mineral deposits occur in six seismically active fracture zones roughly parallel to the axis of the Peru-Chile trench (Carachas-Portillo, Choquelimpie, Iquique, Domeyko, Río Blanco-Los Bayos and Farellones F.Z.), in six fracture zones roughly perpendicular to the trench (El Salvador, Maricunga, Jaroma, Ujina, Tumbaya and Incahuasi-León Muerto F.Z.) and in two fracture zones oriented at an angle of about 45° in relation to the direction of the presently active Andean subduction (Aconcagua and Sierra del Volcán F.Z.). The occurrences of large mineral deposits of different ages show that these fracture zones were also active in the geological past and represent sites of permanent reopening of paths allowing ore-bearing solutions and long-term accumulation of large amounts of metals to occur in relatively restricted domains of the Earth's crust. The mining districts with dated mineral deposits are arranged into four periods of hypogene mineralization: Upper Miocene-Pliocene, Upper Oligocene-Middle Miocene, Upper Eocene-Middle Oligocene, Lower Paleocene-Upper Eocene. These periods of metallogenic activity correlate well with four supposed Andean subduction cycles active in the Tertiary. The occurrence of mineral deposits of different ages in recently active fracture zones can be used as an important evidence in favour of long-term spatial permanence and activity of these zones and as a guide for the discovery of further mineral deposits hidden under young sedimentary and volcanic cover in the fracture zones.

V. Hanuš (✉) · J. Vaněk · A. Špičák
Laboratory of Global Tectonics and Metallogeny,
European Centre Prague, c/o Geophysical Institute,
Academy of Sciences of the Czech Republic,
Boční II/1401, 141 31 Praha 4, Czech Republic
e-mail: hanus@ig.cas.cz

Introduction

The concept of plate tectonic theory has substantially influenced all branches of geoscience, bringing new views not only on deep structures and tectonic evolution but also on the metallogeny of convergent plate margins. After the advent of plate tectonics, several papers describing the spatial and genetic relations between the distribution of mineral deposits and active subduction zones were published (Sillitoe 1972, 1974, 1976; Mitchell 1973; Mitchell and Beckinsale 1982; Frutos 1982). It was shown that mineral deposits at convergent plate margins are genetically connected to processes accompanying the subduction of oceanic lithospheric plates. However, the conclusions are usually of general character, and do not include detailed information on the morphology of the subduction zone and on the tectonic pattern of the overlying continental wedge. Whereas the subduction zone seems to be the primary generator of metallogenic processes at convergent plate margins, the tectonic pattern of the continental wedge appears to channel ore-bearing fluids and to control the deposition of large accumulations of metals.

Over the last decades numerous studies concerning the genesis and age of formation of porphyry and other copper deposits (Sillitoe 1972, 1977, 1981, 1988, 1992; Francis et al. 1983; Ericksen et al. 1986; Skewes and Stern 1994; Gustafson and Quiroga 1995; Marschik et al. 1997), porphyry gold deposits (Sillitoe 1991, 1992, 1997; Sillitoe et al. 1991; Vila and Sillitoe 1991; Vila et al. 1991; McKee et al. 1994; Marschik et al. 1997), epithermal gold-silver-copper deposits (Jannas et al. 1990; Gröpper et al. 1991; Camus and Skewes 1991; Davidson and Mpodozis 1991) and epithermal polymetallic deposits (Ericksen et al. 1986; Fletcher et al. 1989) were carried out in Andean South America.

Detailed studies of the geometry of the distribution of earthquake foci at convergent plate margins reveal that the process of subduction is generally accompanied by a relatively high seismicity in the overlying continental wedge (Hanuš and Vaněk 1977–78, 1983, 1984, 1987, 1992, 1996). It appears that practically all these earthquakes are not distributed randomly but show a clear tendency to accumulate in seismically active fracture zones. These zones can be interpreted as systems of deep seismically active fractures induced or activated in the overlying plate by the process of subduction.

The system of such seismically active fracture zones in the central part of Andean South America was described in Hanuš et al. (1996) and Vaněk et al. (1999). The aim of the present study is to correlate the distribution of large hypogene mineral deposits in the northern and central part of Chile and in the northwestern part of Argentina with the mentioned system of seismically active fracture zones.

Sources of data

For the delineation and construction of the fracture zones in the central part of Andean South America, International Seismological Centre (ISC) data (Regional Catalogue of Earthquakes, 1964–93) were used as the basic material (for details see Hanuš et al. 1996, Vaněk et al. 1999).

The data for the distribution of mineral deposits were taken from Ulriksen (1990) for the northern and central part of Chile and from Mapa Minero (1966) for the northwestern part of Argentina. For the correlation with the seismic data the hypogene polymetallic, copper, gold, lead, silver, tungsten, molybdenum and bismuth deposits in the region between 18°S and 34°S were selected. The mineral deposits in Chilean territory are also classified according to their size. First of all, the mining districts containing mineral deposits classified as very large (*muy grande*) and large (*grande*) in Ulriksen (1990) were considered. A similar size classification system is not available for deposits in Argentina. Therefore, larger clusters of mineral occurrences and deposits, mainly referred to as operating in 1966, were used. These deposits were supplemented by occurrences where age estimations were available. Basic geological and tectonic information was obtained from Mapa Geológico de Chile (1982) and Mapa Geológico de la República Argentina (1982).

Morphology of the subduction zone and seismically active fracture zones

High seismic activity in the region bounded by latitudes 18°S and 34°S allowed us to construct a dense system of vertical cross sections (25 km wide individual sections) perpendicular to the axis of the Peru–Chile trench, which enabled us to distinguish between earthquakes occurring in the subsiding oceanic lithosphere and those situated in the overlying continental plate. As examples, two sections B4 and B33 are shown in Fig. 1 where the Wadati-Benioff zone is delineated by solid parallel lines. Thus, geometric parameters (thickness, dip, depth of penetration) of the subduction zone could be estimated in the whole region investigated. The distribution of earthquakes within the subducted lithopheric plate points to the existence of a distinct aseismic gap, the depth of which varies laterally around 150 km (Hanuš and Vaněk 1976, 1978; Delouis et al. 1996). This gap spatially correlates with the position of active calc-alkaline volcanism. It may indicate possible partial melting of the descending oceanic lithosphere and represent the primary source of magma for active calc-alkaline volcanism. At the same time, the decreased viscosity due to the partial melting of the lithospheric material would exclude the accumulation of stress as the necessary condition of seismic activity (Hanuš and Vaněk 1985). The Andean active volcanic belt is interrupted in several areas where the slab does not reach a sufficient depth due to lateral variations of the depth of penetration of the oceanic plate; in these areas also no aseismic gap is observed in the Wadati-Benioff zone (Hanuš and Vaněk 1978). It seems that these lateral variations show a segmentation of the present subduction zone suggested by several authors (e.g. Sillitoe 1974; Dewey and Lamb 1992).

The earthquake foci above the subduction zone (see Fig. 1) are situated in the South American plate and give evidence of the existence of seismically active fracture

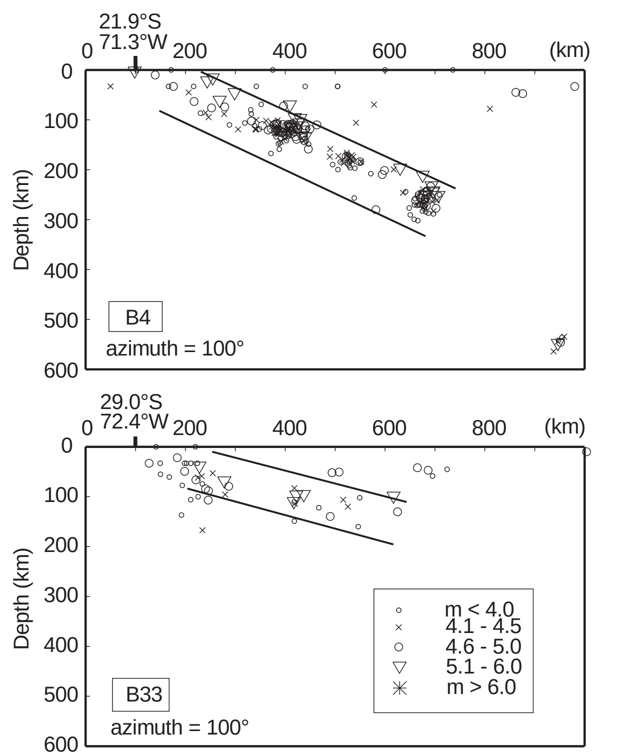

Fig. 1 Vertical sections B4 and B33 with foci of all earthquakes showing the delineation of the Wadati-Benioff zone (*solid parallel lines*) from the continental wedge, *m* indicates ISC earthquake magnitude

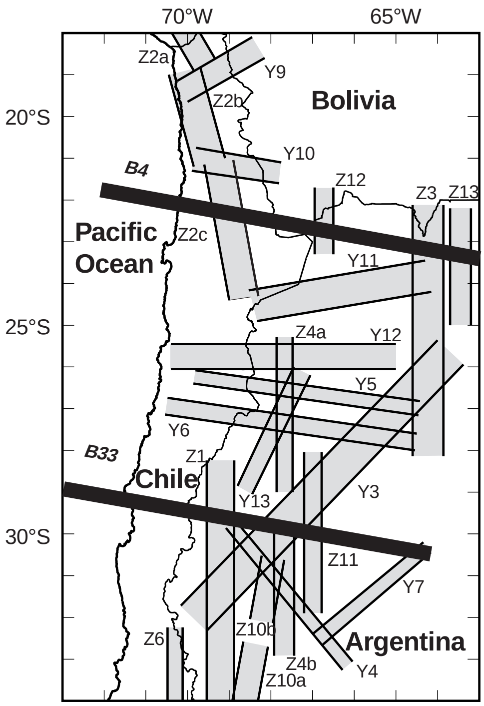

Fig. 2 Pattern of seismically active fracture zones in the continental wedge between 18°S and 34°S and position of sections *B4*, *B33* given in Fig. 1

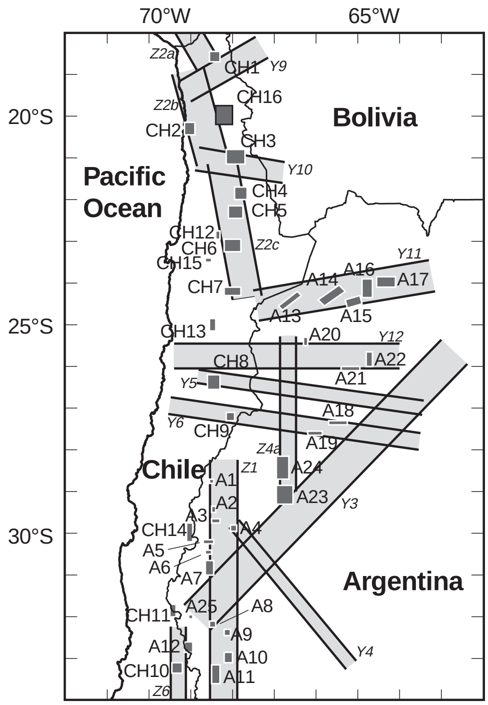

Fig. 3 Distribution of Andean mining districts, denoted by *full rectangles*, in the framework of seismically active fracture zones (for details and names of fracture zones and mining districts see Table 1 and text)

zones in the continental wedge. Between 18°S and 34°S 24 seismically active fracture zones were delineated. The traces of these fracture zones are shown in Fig. 2. The mineralization directly connected with the process of subduction is probably concentrated in the upper part of the overlying plate between the trench and the position of the aseismic gap. This region is situated between 68°W and 71°W for the presently active subduction zone and only 18 fracture zones from the whole set could participate in the process of formation of mineral deposits caused by the Andean subduction (fracture zones Z1, Z2a, Z2b, Z2c, Z4a, Z4b, Z6, Z10a, Z10b, Y3, Y4, Y5, Y6, Y9, Y10, Y11, Y12, Y13). This does not mean that the mineral deposits considered later were necessarily formed during the present subduction. The question of possible preservation of fracture zones activated in the continental lithosphere during several cycles of subduction is discussed later.

Correlation of mineral deposits with seismically active fracture zones

The locations of the hypogene polymetallic, copper, gold, silver, tungsten, molybdenum and bismuth deposits and the system of seismically active fracture zones in the area 18°S–34°S and 65°W–71°W are shown in Fig. 3. The numbered quadrangles represent individual mining districts listed in Table 1. It appears that the mineral deposits occur in the outcrops of the following fracture zones: Carachas-Portillo F.Z. (Z1), Choquelimpie F.Z. (Z2a), Iquique F.Z. (Z2b), Domeyko F.Z. (Z2c), Río Blanco-Los Bayos F.Z. (Z4a), Farellones F.Z. (Z6), Aconcagua F.Z. (Y3), Sierra del Volcán F.Z. (Y4), El Salvador F.Z. (Y5), Maricunga F.Z. (Y6), Jaroma F.Z. (Y9), Ujina F.Z. (Y10), Tumbaya F.Z. (Y11), Incahuasi-León Muerto F.Z. (Y12). These fracture zones can be divided into the following three groups: (1) fracture zones roughly parallel to the trench (Z1, Z2a, Z2b, Z2c, Z4a, Z6), (2) fracture zones roughly perpendicular to the trench (Y5, Y6, Y9, Y10, Y11, Y12), (3) fracture zones oblique to the trench, which are oriented at an angle of about 45° in relation to the direction of the recent Andean subduction (Y3, Y4).

In the following, the main parameters (azimuth, dip, maximum depth) of individual fracture zones are given: Carachas-Portillo F.Z. (Z1), 0°, 65° to E, 80 km, Choquelimpie F.Z. (Z2a), 150°, 60° to NE, 100 km, Iquique F.Z. (Z2b), 165°, 45° to NE, 100 km, Domeyko F.Z. (Z2c), 170°, 50° to NE, 120 km, Río Blanco-Los Bayos F.Z. (Z4a), 0°, 85° to E, 100 km, Farellones F.Z. (Z6), 0°, 60° to E, 40 km, Aconcagua F.Z. (Y3), 45°, 50° to NW, 100 km, Sierra del Volcán F.Z. (Y4), 140°, 65° to NE, 70 km, El Salvador F.Z. (Y5), 100°, vertical, 200 km, Maricunga F.Z. (Y6), 100°, vertical, 190 km, Jaroma F.Z. (Y9), 60°, 50° to SE, 100 km, Ujina F.Z. (Y10), 100°, 60° to N, 100 km, Tumbaya F.Z. (Y11), 80°, 70° to NNW, 140 km, Incahuasi-León Muerto F.Z. (Y12), 90°, 65° to S, 100 km. It should be noted that the reliability of the geometric parameters of the fracture zones (especially of the dip and depth) is limited by the accuracy of the ISC parameter determinations used in this study; however, it is evident that the fracture zones pass through the whole continental lithosphere.

The most important fracture zones Z2a, Z2b, Z2c, Z1, Z6, Z4a, Y11 are shown in Figs. 4–10. For every fracture zone its trace in the map (a), the vertical section across (b) and along (c) the fracture zone with associated earthquakes are given. In the outcrops of the fracture zones the individual faults recorded in the geologic and tectonic maps are shown with the position of the individual mining districts. The faults observed on the surface roughly follow the azimuth of the respective fracture zone.

In the following, tabular summary of the position and mineralization of the mining districts in the system of seismically active fracture zones and the available ages and genetic type of individual deposits are given:

CH1	*Belen-Choquelimpie*	Two groups of polymetallic deposits situated on the crossing of Choquelimpie F.Z. (Z2a) and Jaroma F.Z. (Y9). The Choquelimpie epithermal Ag-Au-Pb-Zn deposit is represented by hydrothermal breccias hosted in a subalkalic stratovolcano of late Miocene age of 6.6 Ma (Gröpper et al. 1991)
CH2	*Iquique*	Group of polymetallic deposits situated near the western boundary of the central part of Iquique F.Z. (Z2b)
CH3	*Ujina*	Group of polymetallic deposits, the large Copaquire Mo deposit and the large Quebrada Blanca Cu, Mo deposit situated on the crossing of Domeyko F.Z. (Z2c) and Ujina F.Z. (Y10). The age of the Quebrada Blanca porphyry copper deposit is 38–36 Ma (Davidson and Mpodozis 1991; Sillitoe 1991) and of the Copaquire Mo deposit 37–34 Ma (Davidson and Mpodozis 1991)
CH4	*San José del Abra*	Group of polymetallic, Au and Cu deposits, the large Guanchaca Ag, Pb deposit and the large El Abra Cu, Mo, Au deposit situated near the eastern boundary of Domeyko F.Z. (Z2c). The age of the El Abra high sulfidation porphyry copper deposit, accompanied by veins striking SE from the porphyry body, is given as 38–37 Ma (Sillitoe 1991), 36–34 Ma (Sillitoe and McKee 1996), 34–33 Ma (Davidson and Mpodozis 1991)
CH5	*Chuquicamata*	Group of polymetallic, Au and Cu deposits, the large Chuqui Norte Cu deposit and the large Chuquicamata Cu, Mo, Ag deposit situated in the central part of Domeyko F.Z. (Z2c). The age of the Chuquicamata porphyry copper deposit is given at 36–31 Ma (Sillitoe and McKee 1996) and 35–28 Ma (Davidson and Mpodozis 1991), the age of supergene oxidation and enrichment of this deposit is 19–15 Ma (Sillitoe and McKee 1996)
CH6	*Caracoles*	Group of Ag and Cu deposits, the large Gran Corrida Ag deposit and the large Centinela Cu deposit situated in the central part of Domeyko F.Z. (Z2c). The age of the Centinela porphyry copper deposit is 44 Ma (Davidson and Mpodozis 1991)
CH7	*La Escondida*	Group of Ag and Cu deposits and the large La Escondida Cu, Mo deposit situated in the southern part of Domeyko F.Z. (Z2c). The age of the La Escondida porphyry copper deposit with related high-sulfidation Cu, Au (Sillitoe 1991) is given as 35–31 Ma (Sillitoe and McKee 1996), 34–31 Ma (Davidson and Mpodozis 1991)
CH8	*El Salvador-Potrerillos*	Group of polymetallic, Cu and Au deposits with the large El Salvador Cu, Mo deposit, the large Potrerillos Cu, Mo, Pb, Au deposit and the large El Hueso Au deposit situated in the western part of the outcrop of El Salvador F.Z. (Y5). The age of the El Salvador porphyry copper deposit, accompanied by an intense vein mineralization of five stages (Gustafson and Quiroga 1995), is 43–31 Ma (Sillitoe and McKee 1996), 42–39 Ma (Davidson and Mpodozis 1991), the age of supergene oxidation and enrichment of this deposit is 23 Ma (Sillitoe and McKee 1996). The Potrerillos porphyry copper deposit is hosted by sedimentary rocks which contain the El Hueso epithermal gold deposit generated at the same time as the porphyry intrusion and associated copper mineralization (Davidson and Mpodozis 1991). The age of the Potrerillos deposit is 35 Ma (Sillitoe and McKee 1996), 38–34 Ma (Davidson and Mpodozis 1991) and the age of the El Hueso deposit is 38–37 Ma (Davidson and Mpodozis 1991)
CH9	*Marte*	Group of Au deposits with the large Marte and Refugio Au deposits situated in the western part of the outcrop of Maricunga F.Z. (Y6). The deposits of this group belong to the Maricunga metallogenic belt. The age of the Marte Au deposit, bound to the quarts – (specularite -magnetite) porphyry stockwork (Vila and Sillitoe 1991, Vila et al. 1991), is 14–13 Ma (Sillitoe 1991), 12 Ma (Davidson and Mpodozis 1991), and of the Lobo Au deposit, bound to the quartz-(specularite-magnetite) porphyry stockwork (Vila and Sillitoe 1991), is 13 Ma (Vila and Sillitoe 1991). The age of the La Pepa Au deposit, bound to the quartz-magnetite porphyry stockwork (Vila and Sillitoe 1991), is given at 23–22 Ma (Sillitoe 1991; Vila and Sillitoe 1991) and of the Refugio Au deposit, bound to the quartz-magnetite-(specularite) porphyry stockwork (Vila and Sillitoe 1991), is given at 23 Ma (Sillitoe 1991; Vila and Sillitoe 1991), 22 Ma (Davidson and Mpodozis 1991)
CH10	*Farellones*	Group of polymetallic deposits with the large Bronces del Río Blanco Cu, Mo deposit and the large La Fortuna Ag, Pb deposit situated in Farellones F.Z. (Z6). The age of the Bronces del Río Blanco porphyry copper deposit is 5–4 Ma (Sillitoe 1991)
CH11	*Los Pelambres*	Group of Cu, Ag deposits with the large Los Pelambres Cu, Mo deposit situated in the northern prolongation of Farellones F.Z. (Z6) and in the southwestern prolongation of Aconcagua F.Z. (Y3). The age of the Los Pelambres porphyry copper deposit based on hydrothermal biotite in diorite porphyry is 9.8 Ma (Sillitoe 1977)
CH12	*Sierra Gorda*	Group of Cu, Au, Ag deposits situated near the western boundary of Domeyko F.Z. (Z2c). The age of the Faride low sulfidation epithermal silver-gold vein deposit (Camus and Skewes 1991) is 64–60 Ma (Sillitoe 1991), 64 Ma (Davidson and Mpodozis 1991). The age of the Catalina Cu, Mo deposit is given at 64–63 Ma and the age of supergene oxidation and enrichment of this deposit at 14 Ma (Sillitoe and McKee 1996)

CH13	*Guanaco*	Group of Au, Ag, Cu deposits situated in the western prolongation of Tumbaya F.Z. (Y11). The age of the El Guanaco high sulfidation epithermal gold-copper-silver vein deposit is 49 Ma (Sillitoe 1991). The age of the Cachinal del la Sierra epithermal silver – (gold) deposit is given at 59–56 Ma (Davidson and Mpodozis 1991)
CH14	*Indio*	Group of Au, Cu, Ag deposits with the large El Indio Au, Cu deposit situated west of Carachas-Portillo F.Z. (Z1) in the northern prolongation of Farellones F.Z. (Z6). The age of the El Indio high sulfidation epithermal gold-silver-copper vein deposit (Jannas et al. 1990; Sillitoe 1991) is 13–8 Ma (Sillitoe 1991), 11–9 Ma (Davidson and Mpodozis 1991)
CH15	*Lomas Bayas*	Group of Cu and Ag, Pb, Cu deposits situated west of Domeyko F.Z. (Z2c). The age of the Lomas Bayas porphyry copper deposit is 61 Ma (Davidson and Mpodozis 1991) and the age of the Fortuna porphyry copper deposit with polymetallic veins is given at 64 Ma (Davidson and Mpodozis 1991)
CH16	*Cerro Colorado*	Group of Cu, Au, Mo and polymetallic deposits situated at the eastern boundary of Iquique F.Z. (Z2b). The age of the Cerro Colorado porphyry copper deposit is 58 Ma (Sillitoe 1991)

A1	*Cordillera de Carachas*	Group of polymetallic deposits situated near the western boundary of Carachas-Portillo F.Z. (Z1)
A2	*Valle del Cura*	Group of polymetallic deposits situated near the western boundary of Carachas-Portillo F.Z. (Z1)
A3	*Cordillera Nevada de Colangüil*	Group of Cu, Ag, W deposits situated near the western boundary of Carachas-Portillo F.Z. (Z1)
A4	*Sierra del Volcán*	Group of Au vein deposits situated at the crossing of Carachas-Portillo F.Z. (Z1) and Sierra del Volcán F.Z. (Y4)
A5	*Cordillera de Conconta*	Group of W, Cu, Mo and polymetallic deposits situated near the western boundary of Carachas-Portillo F.Z. (Z1).
A6	*Cordillera de Olivares*	Group of W, Mo, Au and polymetallic deposits situated near the western boundary of Carachas-Portillo F.Z. (Z1). The age of the Chita W-bearing porphyry copper deposit based on biotite from andesite porphyric stock is 11.7 Ma (Sillitoe 1977, 1981)
A7	*Rio Castaňo*	Group of Cu, Au, Bi and polymetallic deposits with the operated Cuatro Amigos polymetallic deposit and Castaňo Nuevo Au deposit situated near the northern crossing of Carachas-Portillo F.Z. (Z1) and Aconcagua F.Z. (Y3)
A8	*Cordillera del Tigre*	Group of Cu deposits with the operated Cantera el Angelito, Cantera el Rincón and Don León deposits situated at the southern crossing of Carachas-Portillo F.Z. (Z1) and Aconcagua F.Z. (Y3)
A9	*Cordillera Cortaderas*	Group of Au, Cu and polymetallic deposits with the operated Mantos de Cobre Cu deposit and Paramillos de Uspallata polymetallic deposit situated near the eastern boundary of Carachas-Portillo F.Z. (Z1). The age of the Paramillos Norte porphyry copper deposit based on hydrothermal muscovite in sericitized latite porphyry is given as 16 Ma (Sillitoe 1977, 1981)
A10	*Guido*	Group of Cu and polymetallic deposits with the operated San Lorenzo Cu deposit and Los Mantos Preciosos polymetallic deposit situated near the eastern boundary of Carachas-Portillo F.Z. (Z1)
A11	*Cordón Portillo*	Group of many Cu, Au, W, Mo and polymetallic deposits with the operated Salamanca Cu deposit situated near the western boundary of Carachas-Portillo F.Z. (Z1)
A12	*Aconcagua*	Group of Cu deposits situated at the crossing of Farellones F.Z. (Z6) and prolongated Aconcagua F.Z. (Y3). The age of one porphyry copper deposit in the Río de las Vacas complex based on hydrothermal biotite in potassium silicate altered granodiorite porphyry is 8.5 Ma (Sillitoe 1977, 1981)
A13	*Taca Taca*	Group of Cu deposits situated in the central part of Tumbaya F.Z. (Y11)
A14	*San Antonia de los Cobres*	Group of polymetallic and Cu deposits with the operated Elvira polymetallic deposit situated in the central part of Tumbaya F.Z. (Y11)
A15	*Meseta*	Group of polymetallic and Cu deposits with the operated Diana polymetallic deposit situated near the southern boundary of Tumbaya F.Z. (Y11)
A16	*Sierra de Chaňi*	Group of polymetallic, Au and Cu deposits situated in Tumbaya F.Z. (Y11)
A17	*Tumbaya*	Group of polymetallic and Cu deposits with the operated Chorrillos and María Remedios Cu deposits situated in the central part of Tumbaya F.Z. (Y11). The age of the Pancho Arías porphyry copper deposit based on hydrothermal biotite in potassium silicate altered dacite porphyry is given as 15.4 Ma (Sillitoe 1977, 1981)
A18	*Capillitas*	Group of Au, Ag and Cu deposits with the operated Carmelitas Cu deposit situated at the northern boundary of Maricunga F.Z. (Y6). The age of four different porphyry copper deposits (Bajo del Durazno, Bajo de Pampitas, Bajo de San Lucas, Mi Vida) based on biotite in potassium silicate altered andesite and monzonite porphyry is 7.9–6.8 Ma (Sillitoe 1977, 1981)

A19	*Belen*	Group of W deposits at the southern boundary of Maricunga F.Z. (Y6)
A20	*Incahuasi*	Group of Au deposits situated at the northern boundary of Incahuasi-León Muerto F.Z. (Y12). The age of the Inca Viejo porphyry gold deposit based on magmatic biotite in dacite porphyry is given at 15 Ma (Sillitoe 1977, 1981)
A21	*Cafayate*	Group of Cu deposits situated at the southern boundary of Incahuasi-León Muerto F.Z. (Y12)
A22	*León Muerto*	Group of Cu deposits with the operated El Zorrito, Margarita and Zorriquín deposits situated at the southern boundary of Incahuasi-León Muerto F.Z. (Y12)
A23	*Los Bayos-El Tigre*	Group of Cu, Au and polymetallic deposits with the operated San Sebastian Cu deposit situated at the crossing of Río Blanco-Los Bayos F.Z. (Z4a) and Aconcagua F.Z. (Y3). The age of the Los Bayos porphyry copper deposit based on biotite from pre-mineral quartz diorite intrusive is 5.7 Ma (Sillitoe 1981)
A24	*Mogote Río Blanco*	Group of Cu, Au and polymetallic deposits with the operated Monte Verde and Santa María Cu, Au deposits situated at the western boundary of Río Blanco-Los Bayos F.Z. (Z4a). The age of porphyry copper-gold deposits with associated polymetallic mineralization in this district is given as 8 Ma (Sillitoe 1997)

Table 1 contains the list of individual mineral occurrences; the numbering of Chilean occurrences in mining districts CH1–CH16 was taken from Ulriksen (1990), numbering of Argentinean occurrences for mining districts A1–A7 from Mapa Minero of San Juan, A8–A12 from Mapa Minero of Mendoza, A13–A17 and A21–A22 from Mapa Minero of Salta y Jujuy, A18–A20 from Mapa Minero of Catamarca y Tucuman and A23–A24 fr om Mapa Minero of La Rioja. The mining districts mentioned represent practically all important accumulations of metals given in the above maps for the region studied. The newly discovered porphyry Cerro Mercedario copper deposit, denoted in Fig. 3 as A25, is situated in the northern prolongation of Farellones F.Z (Z6) and in the southwestern prolongation of Aconcagua F.Z. (Y3); its age, based on hydrothermal biotite in quartz monzonite porphyry, is 13 Ma (Sillitoe 1977, 1981). The age of the large E1 Teniente porphyry copper deposit, situated several kilometres south of 34°S in the central part of Farellones F.Z (Z6), is given at 5.6–4.3 Ma (Sillitoe 1981). The Cretaceous Andacollo, Los Mantos de Punitaqui and E1 Bronce deposits (Sillitoe 1991) were not considered because they do not belong to manifestations of the last system of subduction cycles (Soler and Bonhomme 1988).

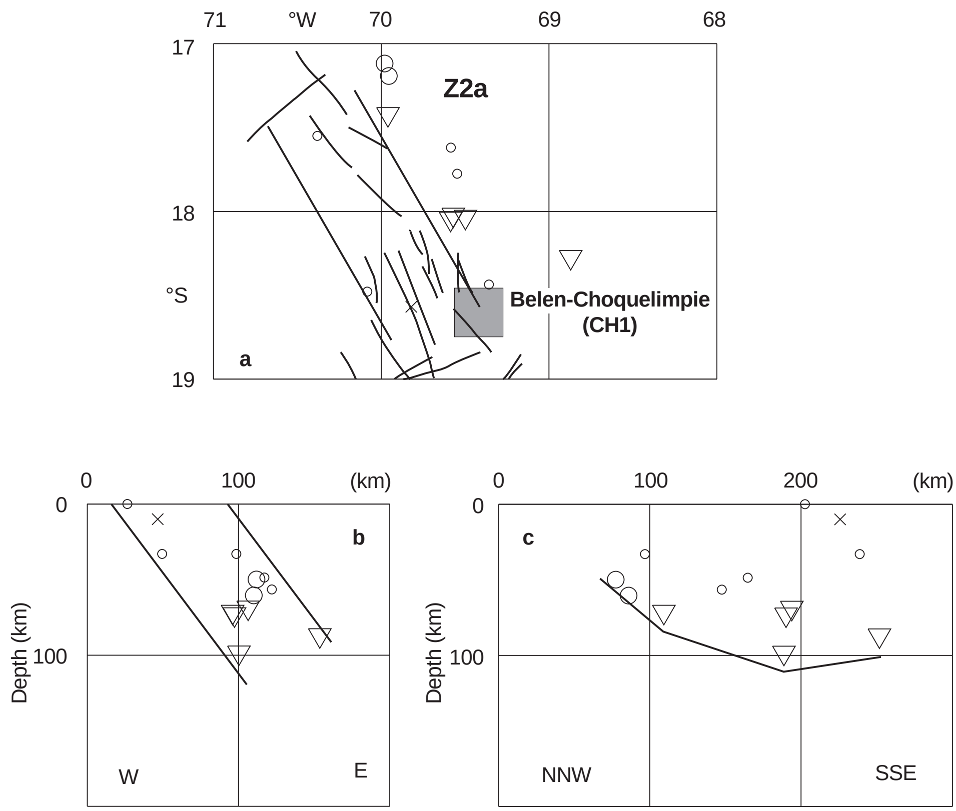

Fig. 4a–c Location of the Choquelimpie fracture zone *Z2a* with associated earthquakes **a**, transverse section **b** across and longitudinal section **c** along the fracture zone; faults observed on the surface are denoted by *lines* and numbered mining districts by *shaded rectangles* (for details see Table 1). *Symbols* of earthquakes as in Fig. 1

Table 1 List of Andean mining districts between 18°S and 34°S situated in the outcrops of seismically active fracture zones

District	Area (S, W)	Occurrences	Type of mineralization
CH1	Belen-Choquelimpie 18.3, 69.55; 18.7, 69.55; 18.3, 69.3; 18.7, 69.3	27 Choquelimpie N.	Ag, Au, Pb, Zn
		28 Choquelimpie S.	Ag, Pb, Zn
		32 Patiňo	Ag, Pb, Zn, Cu
		37 Campanani	Ag, Pb, Zn
		40 Santa Rosa	Ag, Pb, Zn
		42 Churicala Norte	Cu, Ag
		43 Chulpa	Ag, Pb, Zn
		44 Capitana	Ag
		45 Ociel	Ag, Sb
CH2	Iquique 20.15, 70.15; 20.45, 70.15; 20.15, 69.9; 20.45, 69.9	10 Juana	Au, Ag, Pb
		11 Pajonales	Ag, Cu, Pb
		12 Westfalia	Cu
		27 Huantajaya	Ag, Cu, Pb, Zn
		28 Socavón	Ag, Pb, Cu
		29 Rosa Amelia	Ag, Pb, Cu
		30 NN4	Ag, Pb
		32 Consuelo	Cu, Au
		33 Rosario	Cu, Ag, Pb
		34 Gran Veta	Ag, Pb, Cu
		35 El Godo	Ag, Pb
		37 Atahualpa	Ag, Pb
CH3	Ujina 20.8, 69.15; 21.15, 69.15; 20.8, 68.7; 21.15, 68.7	60 Copaquire (large)	Mo
		61 Flor de Tarapacá	Ag, Pb, Cu
		62 Malta	Mo
		63 Colcol	Ag, Pb, Cu
		72 Catigna	Cu
		73 Las Porfiadas	Cu
		74 Yamincha	Cu
		4 Quebrada Blanca (large)	Cu, Mo
		5 Yareta	Ag, Au, Mn
		6 Jovita	Cu
		7 Trinidad	Ag, Mn
		8 Montezuma	Au, Cu, Mn
		11 Anita	Cu, Au
		12 Quilahueňa	Cu, Au
		13 Pirula	Ag, Pb
		14 Capona	Au, Ag, Cu
		15 Olga	Cu, Au
CH4	San José del Abra 21.7, 68.95; 22.0, 68.95; 21.7, 68.65; 22.0, 68.65	31 Arco	Pb
		32 Vizcachilla	Cu
		33 Mal Paso	Au
		34 Aguadita	Ag, Pb, Zn
		35 Guanchaca (large)	Ag, Pb
		46 Sajasa	Au
		47 Sin Nombre	Cu
		48 El Abra (large)	Cu, Mo, Au
		49 Gral. Baquedano	Cu, Ag
		55 Colpa	Cu, Au, Ag
CH5	Chuquicamata 22.15, 69.1; 22.45, 69.1; 22.15, 68.75; 22.45, 68.75	18 Irene (large)	Ag, Au, Cu
		19 Mujer	Au
		20 Andina	Cu
		21 Tomasol	Cu
		22 Tres Cerros	Ag, Pb
		23 Jarosita	Ag, Pb
		24 Chuqui Norte (large)	Cu
		29 Andacollo	Au, Ag, Cu
		30 Chuquicamata (large)	Cu, Mo, Ag
		36 Sta. Genoveva	Ag, Pb
		40 San Salvador	Ag, Pb
		41 Tres Compadres	Cu
CH6	Caracoles 22.95, 69.2; 23.25, 69.2; 22.95, 68.8; 23.25, 68.8	3 Deseada-Filomena (large)	Ag
		4 Descubridora	Ag
		5 San Luis	Ag

Table 1 Contd.

District	Area		Occurrences	Type of mineralization
	S	W		
			6 Cerro Pedregal	Ag
			7 Gran Corrida de Caracoles	Ag
			8 Luisa	Ag
			9 La Isla	Ag
			16 Centinela (large)	Cu
			17 Los Amigos	Pb, Ag
			18 San José	Cu
CH7	La Escondida		18 Sin Nombre	Ag
	24.1, 69.2; 24.3, 69.2;		19 Alicia	Ag
	24.1, 68.8; 24.3, 68.8		20 Rincones	Ag, Pb
			21 Sin Nombre	Ag
			22 Marisol	Cu, Ag
			23 La Escondida (large)	Cu, Mo
			24 La Casualidad	Cu
CH8	El Salvador-Potrerillos		11 Arenal	Cu
	26.2, 69.6; 26.55, 69.6;		17 Quebrada de las Salinas	Cu, Ag, Au
	26.2, 69.3; 26.55, 69.3		18 El Salvador (large)	Cu, Mo
			51 Potrerillos (large)	Cu, Mo, Pb, Au
			129 El Hueso (large)	Au
CH9	Marte		169 Marte (large)	Au
	27.15, 69.3; 27.45, 69.3;		170 Soledad	Au
	27.15, 69.05; 27.45, 69.05		171 Pepa	Au
			172 Lobo	Au
			173 Escondida	Au
			174 Refugio (large)	Au
			73 Pantanillo	Au
CH10	Farellones		17 Bronces del Río Blanco et al. (large)	Cu, Mo
	33.1, 70.45; 33.35, 70.45;		18 Lomas Bayas	Ag
	33.1, 70.2; 33.35, 70.2		19 La Fortuna (large)	Ag, Pb
			20 Los Sulfatos	Cu, Ag
			29 Victoria et al.	Pb, Cu, Ag
			48 Morena	Cu
CH11	Los Pelambres		121 Los Pelambres (large)	Cu, Mo
	31.7, 70.5; 32.0, 70.5;		154 Primavera-Resguardo	Cu
	31.7, 70.35; 32.0, 70.35		169 El Totoral	Cu, Ag
			170 El Manzano	Cu, Ag
CH12	Sierra Gorda		85 Pampa Lina	Cu
	22.75, 69.4; 22.95, 69.4;		86 Millonaria	Cu
	22.75, 69.3; 22.95, 69.3		87 Faride et al.	Cu, Au, Ag
			88 Catalina et al.	Cu, Mo
			89 La Vendida et al.	Cu, Au, Ag
			90 Copucha	Cu
			91 Bello Cambio	Cu
			92 La Compañía	Cu, Au, Ag
CH13	Guanaco		12 Inesperada	Au, Ag
	24.85, 69.55; 25.15, 69.55;		13 El Guanaco et al.	Au, Cu, Ag
	24.85, 69.4; 25.15, 69.4		61 El Soldado	Ag, Pb
			62 Cachinal de la Sierra	Ag
CH14	Indio		66 El Indio (large)	Au, Cu
	29.75, 70.1; 30.2, 70.1;		98 Las Hediondas	Au
	29.75, 69.95; 30.2, 69.95		11 Carmen	Au, Ag
			164 San Antonio	Cu, Ag, Au
CH15	Lomas Bayas		48 Chicago	Cu
	23.4, 69.65; 23.5, 69.65;		49 La Paloma	Cu
	23.4, 69.5; 23.5, 69.5		50 San Manuel	Cu
			51 Lomas Bayas	Cu
			52 Fortuna	Ag, Pb, Cu
CH16	Cerro Colorado		21 Paguanta	Ag, Pb, Cu
	19.75, 69.4; 20.2, 69.4;		22 Limacsiña	Ag
	19.75, 69.0; 20.2, 69.0		23 Sta. Rita, San Antonio	Ag, Pb, Zn
			24 Beatriz et al.	Cu, Au

Table 1 Contd.

District	Area		Occurrences	Type of mineralization
	S	W		
			25 María Inés, Pascuala	Cu, Au
			26 San Juan de Mocha	Cu, Au
			27 Enrique et al.	Cu, Au, Ag
			28 Subercagua	Ag, Pb, Zn
			29 Sta. Fe	Cu
			30 Colpa	Cu
			31 Mosquito de Oro	Au
			32 Chana, Sta. Rosa	Au, Cu
			39 Violeta	Ag, Pb
			3 Cerro Colorado	Cu, Mo
			4 Amilca	Cu, Au
			5 San Marcos	Cu, Ag, Pb,
			6 Flor del Desierto et al.	Cu, Ag, Pb, Zn
			7 San Andrés	Ag, Pb, Zn
			8 Gualchagua	Cu
			9 Columtucsa	Cu
			13 Molibdeno Cerro Colorado	Cu, Mo
			14 Sagasca	Cu
			15 Mollaca	Cu, Ag
			16 Río Tinto N	Cu
			17 Luisa de Canulpa	Ag, Au, Pb, Zn
			18 Zoila Rosa et al.	Cu, Ag, Pb, Zn, Au
			19 Aguada et al.	Cu, Ag, Pb, Zn
			20 Sofia, Infiernillo	Cu
			21 Labraza, Santiago	Cu
			22 La Planada et al.	Cu, Au, Mo
			23 Sofia	Ag, Au, Pb, Zn
			24 Jauja	Ag, Au, Pb, Zn
			25 Río Tinto S	Cu
			26 Sitilca	Cu, Au
A1	Cordillera de Carachas 28.7, 69.45; 28.8, 69.45; 28.7, 69.55; 28.8, 69.55		1 La Negra 2 La Argentina 3 La Azul 4 Josefina	Pb, Ag, Zn Pb, Ag, Zn Pb, Ag, Zn Pb, Ag, Zn
A2	Valle del Cura 29.35, 69.4; 29.5, 69.4; 29.35, 69.5; 29.5, 69.5		6 La Primera 7 La Segunda 8 Sarmiento 9 Fierro Alto	Pb, Ag, Zn Pb, Ag, Zn Pb, Ag, Zn Pb, Ag, Zn
A3	Cordillera Nevada de Colangüil 29.65, 69.3; 29.75, 69.3; 29.65, 69.5; 29.75, 69.5		12 Judas Tadeo 13 El Salado 15 San José 16 San Joaquín	Cu Ag Cu W
A4	Sierra del Volcán 29.8, 69.05; 29.95, 69.05; 29.8, 68.9; 29.95, 68.9		17 La Punilla 18 Despreciada 82 Los Caballos 83 Guachi	Au Au Au Au
A5	Cordillera de Conconta 30.15, 69.45; 30.25, 69.45; 30.15, 69.7; 30.25, 69.7		24 La Ernestina 25 Don Esteban 26 Conconta 31 San Antonio 32 La Unión 33 Rincón Seco 34 Don Roberto 36 Las Cruces 37 Don Marcos	W W W Cu W Pb, Zn, Ag W W Mo
A6	Cordillera de Olivares 30.4, 69.5; 30.5, 69.5; 30.4, 69.65; 30.5, 69.65		41 Cerro del Bronce, Chita 42 La Majadita 43 Catalina 44 Arqueros 45 San Pablo	W W Pb, Ag, Zn Mo Au
A7	Río Castaño 30.65, 69.45; 31.0, 69.45; 30.65, 69.65; 31.0, 69.65		47 Dos Amigos 48 Flor de los Andes 50 Don Arturo	Cu Bi Cu

Table 1 Contd.

District	Area		Occurrences	Type of mineralization
	S	W		
			51 Reyes Magos	Cu
			53 Amancay	Bi
			54 San Francisco de los Andes	Cu
			55 Castaño Viejo	Pb, Ag, Zn
			56 Cuatro Amigos (active)	Pb, Ag, Zn
			57 Castaño Nuevo (active)	Au
A8	Cordillera del Tigre		105 La Deheza	Cu
	32.1, 69.4; 32.25, 69.4;		106 Cantera el Angelito (active)	Cu
	32.1, 69.55; 32.25, 69.55		107 Cantera el Rincón (active)	Cu
			110 Don León (active)	Cu
A9	Cordillera Cortaderas		79 Boquí	Au
	32.3, 69.05; 32.45, 69.05;		83 Al Fin Hallada	Au
	32.3, 69.2; 32.45, 69.2		85 Mantos de Cobre (active)	Cu
			89 Andacollo	Cu
			91 La Carolina	Au
			92 Brillante	Au
			420 Delirio	Cu
			430 Paramillos de Uspallata (active)	Ag, Pb, Zn
A10	Guido		1 San Pedro Nolasco	Pb, Ag, Zn
	32.85, 69.0; 33.1, 69.0;		2 San Lorenzo (active)	Cu
	32.85, 69.2; 33.1, 69.2		3 La Esperanza	Cu
			13 Atlas	Cu
			25 Doña Ida	Cu
			42 Los Mantos Preciosos (active)	Cu
			45 Juanita	Pb, Ag, Zn
A11	Cordón Portillo		138 La Sarita	Cu
	33.15, 69.3; 33.6, 69.3;		139 Clarita	Cu
	33.15, 69.5; 33.6, 69.5		140 Amelia	Cu
			144 Dora Mercedes	Au
			145 El Cóndor	Au
			146 San Juan	Au
			147 Benita	Cu
			153 Barrera	Cu
			154 Salamanca (active)	Cu
			155 La Serena	Au
			166 La Lola	Au
			167 Blanquita	W
			169 La Toma	W
			173 Alborada	Mo
			174 30 de Agosto	Pb, Ag, Zn
A12	Aconcagua		127 Germinal	Cu
	32.6, 70.15; 32.85, 70.15;		128 El Sol	Cu
	32.6, 69.95; 32.85, 69.95		129 Catalina	Cu
			130 Irica	Cu
			131 San José	Cu
			426 San Sebastián	Cu
A13	Taca Taca		230 Ana	Cu
	24.55, 67.9; 24.65, 67.8;		240 Taca Taca	Cu
	24.2, 67.45; 24.3, 67.35		243 Flamarion	Cu
			468 Marcelo	Cu
			470 Arizaro	Cu
A14	San Antonio de los Cobres		48 Soncaimán	Pb, Zn, Ag
	24.4, 66.95; 24.55, 66.8;		287 Vicuña	Pb, Zn, Ag
	24.05, 66.45; 24.2, 66.3		288 Emilia	Cu
			290 Concordia	Cu
			298 Armonía	Pb, Zn, Ag
			303 Portezuelo	Pb, Zn, Ag
			306 Elvira (active)	Pb, Zn, Ag
			307 California	Pb, Zn, Ag
			488 La Purísima	Pb, Zn, Ag
			489 La Olvidada	Pb, Zn, Ag
			554 Andrómaca	Pb, Zn, Ag

Table 1 Contd.

District	Area S W	Occurrences	Type of mineralization
A15	Meseta 24.4, 66.3; 24.6, 66.25; 24.3, 65.95; 24.5, 65.9	314 Leonor	Cu
		315 Elsa	Cu
		317 Encrucijada	Pb, Ag, Zn
		393 Isa	Cu
		394 Aries	Cu
		395 Gloria	Pb, Ag, Zn
		466 Saturno	Cu
		469 Virgen del Carmen	Cu
		499 San Antonio Abad	Pb, Ag, Zn
		501 Diana (active)	Pb, Ag, Zn
A16	Sierra de Chañi 23.9, 65.9; 24.35, 65.9; 23.9, 65.65; 24.35, 65.65	126 Achacanal	Pb, Ag, Zn
		128 Stella	Pb, Ag, Zn
		129 Palomar	Cu
		130 Antigua	Pb, Ag, Zn
		131 El Porvenir	Pb, Ag, Zn
		386 Ciénaga Redonda	Pb, Ag, Zn
		387 Chañi	Au
		388 San José de Chañi	Cu
		491 San Pedro	Pb, Ag, Zn
A17	Tumbaya 23.85, 65.55; 24.1, 65.55; 23.85, 65.1; 24.1, 65.1	159 Santa María	Pb, Ag, Zn
		161 Oclayas	Pb, Ag, Zn
		163 Yolanda	Pb, Ag, Zn
		164 Gral. Güemes	Pb, Ag, Zn
		166 Chorrillos (active)	Cu
		167 Elsa	Pb, Ag, Zn
		168 La Italiana	Pb, Ag, Zn
		635 Alicia	Cu
		637 León	Pb, Ag, Zn
		638 Cerro Bola	Pb, Ag, Zn
		640 María Remedios (active)	Cu
A18	Capillítas 27.3, 66.7; 27.4, 66.7; 27.3, 66.25; 27.4, 66.25	44 Abel Peirano (Farellón Negro)	Au, Ag
		46 Los Angeles	Au
		47 Virgen del Valle	Cu
		48 Carmelitas (active)	Cu
		49 Agua Rica	Cu
A19	Belen 27.55, 67.2; 27.65, 67.2; 27.55, 66.85; 27.65, 66.85	9 Del Valle	W
		10 El Chincal	W
		51 Luna Aguada	W
A20	Incahuasi 25.3, 67.3; 25.5, 67.3; 25.3, 67.2; 25.5, 67.2	3 Incahuasi et al.	Au
		4 Esperanza et al.	Au
A21	Cafayate 26.0, 66.4; 26.1, 66.4; 26.0, 65.95; 26.1, 65.95	512 Juan Esteban	Cu
		517 Los Cardones	Cu
		518 San Francisco	Cu
		519 Casualidad III	Cu
		539 Don Juan	Cu
A22	León Muerto 25.65, 65.8; 26.0, 65.8; 25.65, 65.65; 26.0, 65.65	414 Deshechos	Cu
		415 San Antonio	Cu
		420 El Zorrito et al. (active)	Cu
		421 Margarita (active) and Zorriquín (active)	Cu
		513 Constelación et al.	Cu
		514 Abundancia et al.	Cu
		540 Tehuelche	Cu
A23	Los Bayos – El Tigre 28.85, 67.95; 29.3, 67.95; 28.85, 67.55; 29.3, 67.55	80 Imma	Cu
		81 La Vegulta	Pb, Ag, Zn
		82 Malaquita et al.	Cu
		83 La Encrucijada	Cu
		84 Los Bayitos	Au
		87 Las Pircas	Cu
		89 Clorinda	Cu

Table 1 Contd.

District	Area		Occurrences	Type of mineralization
	S	W		
			90 Ampallado	Cu
			91 El Pararrayo	Cu
			92 Italia	Cu
			93 San Pedro et al.	Cu
			94 La Aragonesa	Pb, Ag, Zn
			95 La Cobriza	Cu
			96 Los Bayos	Cu
			98 El Tigre	Pb, Ag, Zn
			103 El Oro	Au
			106 San Sebastian (active)	Cu
A24	Mogote Río Blanco		62 Las Amolanas	Pb, Ag, Zn
	28.15, 67.95; 28.7, 67.95;		63 La Alumbrera	Pb, Ag, Zn
	28.15, 67.65; 28.7, 67.65		64 El Cerquito	Pb, Ag, Zn
			65 Nuestra Sra. de Andacollo	Pb, Ag, Zn
			66 Mal Paso	Au
			70 Sotrán	Cu
			71 Monte Verde et al. (active)	Cu, Au
			72 Santa María (active)	Cu, Au

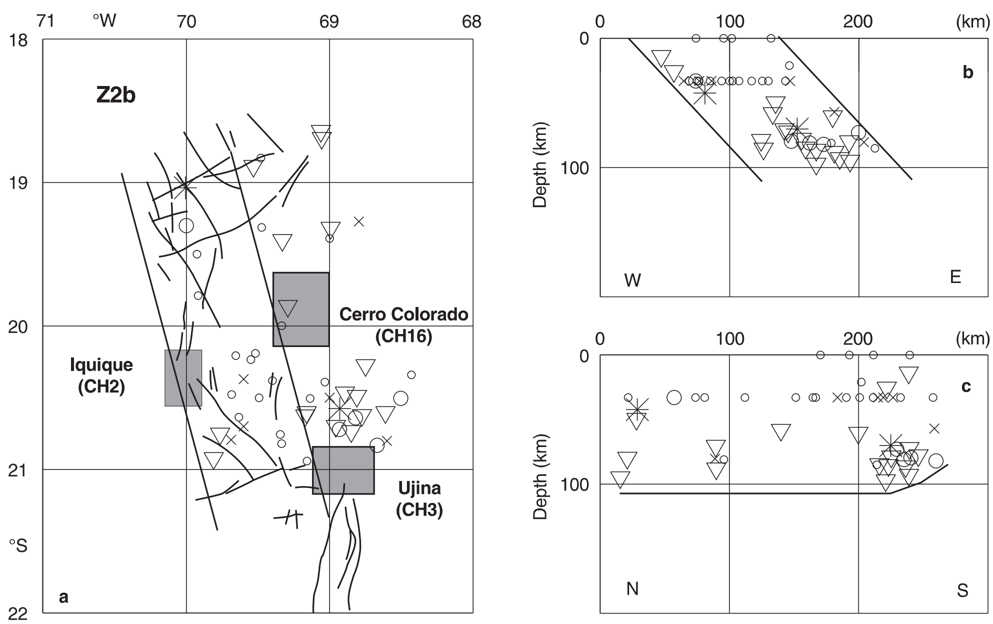

Fig. 5a–c Location of the Iquique fracture zone *Z2b* with associated earthquakes **a**, transverse section **b** across and longitudinal section **c** along the fracture zone. For key see Fig. 4

Discussion

The description and figures indicate that the most important mining districts in the Andean segment between 18°S and 34°S are situated in the outcrops of the seismically active fracture zones related to the present subduction of the Nazca plate. However, the distribution of mineral deposits is not strictly uniform in type, mineral contents and age.

The majority of mineral deposits of porphyry copper type are situated in the Domeyko F.Z. (Z2c), Río Blanco-Los Bayos F.Z. (Z4a), Farellones F.Z. (Z6), and in the east-west trending E1 Salvador F.Z. (Y5) and Maricunga F.Z. (Y6). Polymetallic deposits occur mainly in the Choquelimpie F.Z. (Z2a) Iquique F.Z. (Z2b) and lncahuasi-León Muerto F.Z. (Y12). Polymetallic vein deposits and Cu veins prevail in the Carachas-Portillo F.Z. (Z1).

The available ages of Tertiary magmatic rocks hosting mineral deposits described can be arranged into four periods: A: Upper Miocene-Pliocene, B: Upper Oligocene-Middle Miocene, C:Upper Eocene-Middle Oligocene, D:Lower Paleocene-Upper Eocene (compare

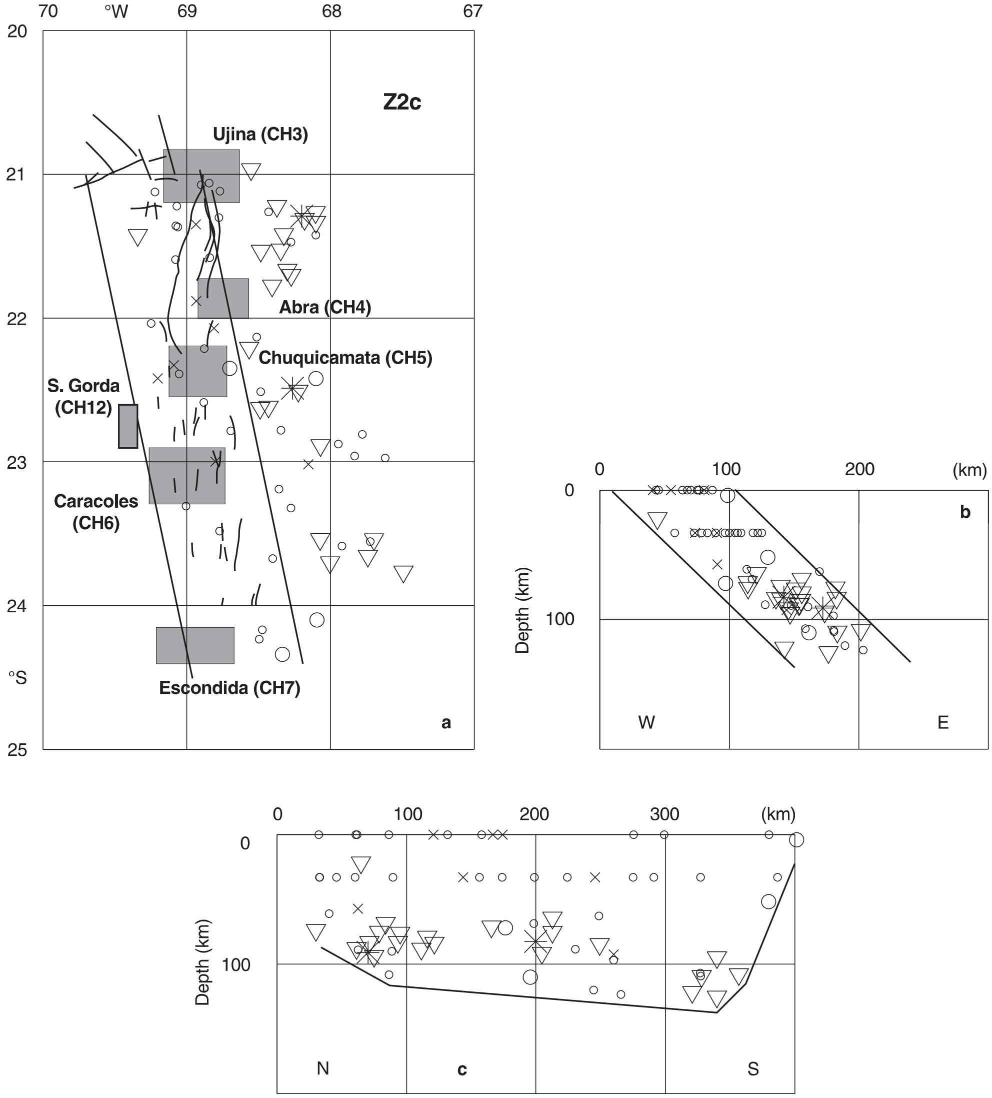

Fig. 6a–c Location of the Domeyko fracture zone *Z2c* with associated earthquakes **a**, transverse section **b** across and longitudinal section **c** along the fracture zone. For key see Fig. 4

Sillitoe 1981; Davidson and Mpodozis 1991). It appears that individual seismically active fracture zones are characterized by the occurrence of mineral deposits of different age. In Table 2 the fracture zones are arranged from north to south according to these time periods.

The distribution of dated mineral deposits and sketches of metallogenic belts of different ages are plotted in the framework of the seismically active fracture zones between 18°S and 34°S in Fig. 11. It should be noted that this picture depends on the availability and accuracy of age determinations. Figure 11 shows that all young manifestations of hypogene metallogeny of period A are situated within the outcrops of the present fracture zones (Z2a, Y6, Z4a, Z1, Z6). This young mineralization is concentrated north of 19°S and south of 27°S and does not occur in the central part of the region between 20°S and 26°S where the metallogenic belts of period C and D are developed mainly in the outcrop and vicinity of Domeyko F.Z. (Z2c). It appears that the deposits of period B are located south of 24°S and do not tend to form clearly defined metallogenic belts. In every case, the considered mineral deposits of all periods are accumulated in the present system of seismically active fracture zones. This distribution of mineral deposits points to the spatial permanency of this system of fracture zones activated by the process of subduction in relation to the western margin of the South American continent since the Lower Paleocene. However, small alterations to this system probably occurred during this time due to specific pecularities of individual subduction cycles.

The hypothesis that the subduction runs in cycles connected with the formation of a system of successive subsiding slabs shifted several tens of kilometres towards or against the direction of the corresponding ocean floor spreading (Hanuš and Vaněk 1991, 1996) seems to have fundamental importance for the formation of large accumulations of metals at convergent plate margins. The continental lithosphere, moving against the direction of

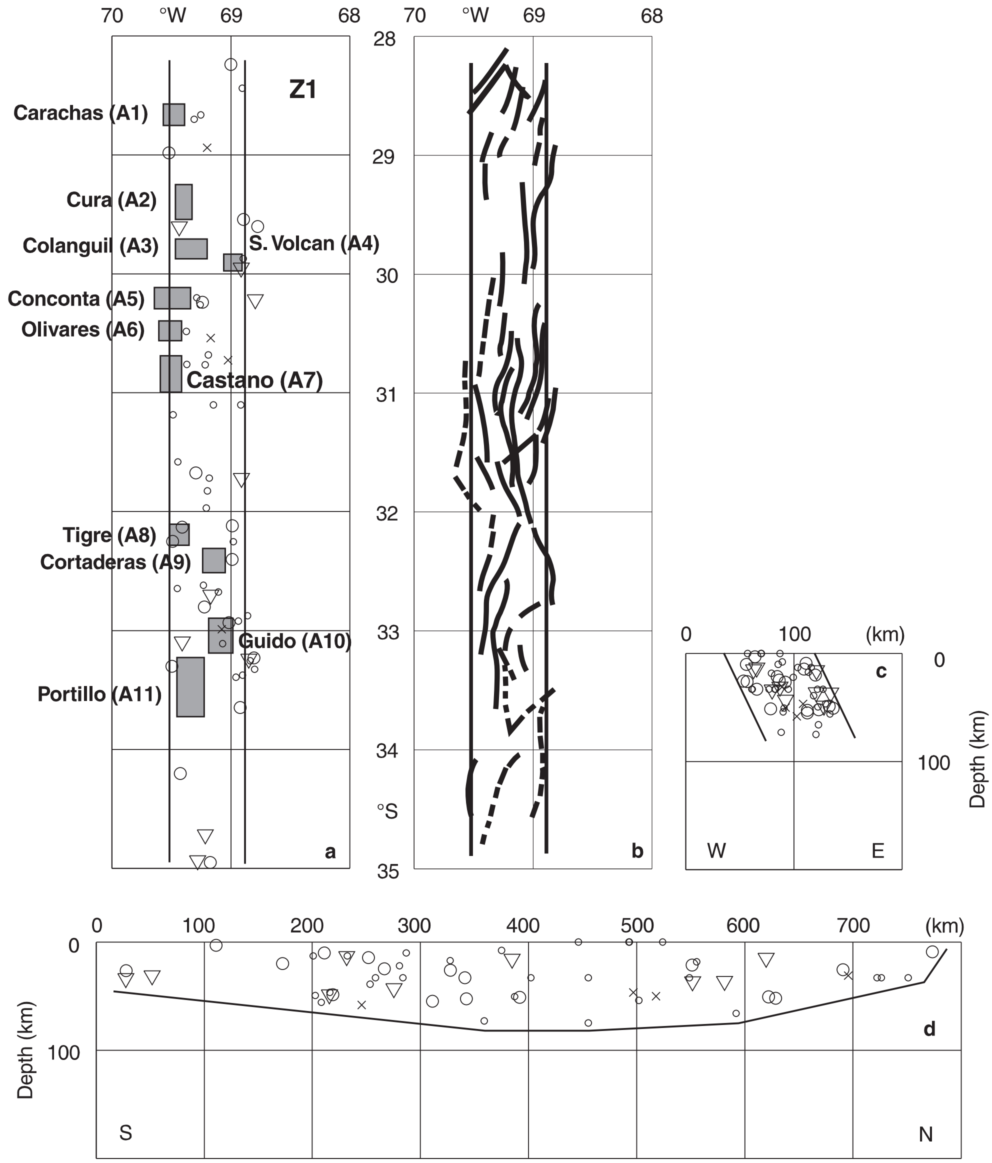

Fig. 7a–d Location of the Carachas-Portillo fracture zone *Z1* with associated earthquakes **a**, faults observed on the surface **b**, transverse section **c** across and longitudinal section **d** along the fracture zone. For key see Fig. 4

the ocean floor spreading, meets subduction zones of different age generated by subsequent cycles of subduction. It appears that the fracturing of the continental lithosphere near the convergent plate boundary, which is shown by the described seismically active fracture zones, remains preserved in time, being re-activated under favourable stress conditions by the sequence of subduction cycles of different age.

In Andean South America, deep earthquakes observed at depths between 500 and 600 km do not geometrically fit the linear prolongation of the present Wadati-Benioff zone (see Fig. 1 and Hanuš and Vaněk 1978, 1991) and we explain their occurrence as a product of an activation of paleoslabs buried in the upper mantle. According to this hypothesis, we suppose that these paleoslabs represent relics of foregoing cycles of subduction activated at the present time. They are not connected to the presently active subduction zone represented by shallow and intermediate earthquakes divided from the belt of deep earthquakes by a broad aseismic region at depths between 300 and 500 km (Hanuš and Vaněk 1976, 1991).

If we try to apply this hypothesis of cyclic development of subduction to the region of Andean South America between 18°S and 34°S, we arrive at the following model of the subduction history: The observed shape of the present Wadati-Benioff zone shows that in this region the maximum depth of penetration of the oceanic lithophere beneath the South American continent laterally varies up to 250–300 km (Cahill and Isacks 1992), which corresponds to a length of 600–700 km at the observed dip of the present subduction zone. Considering the rate of 6 cm/y for the subduction of the Nazca plate (Corvalan 1981), the duration of the present subduction would be 10–12 Ma. Because a completed cycle of subduction, given by the maxi-

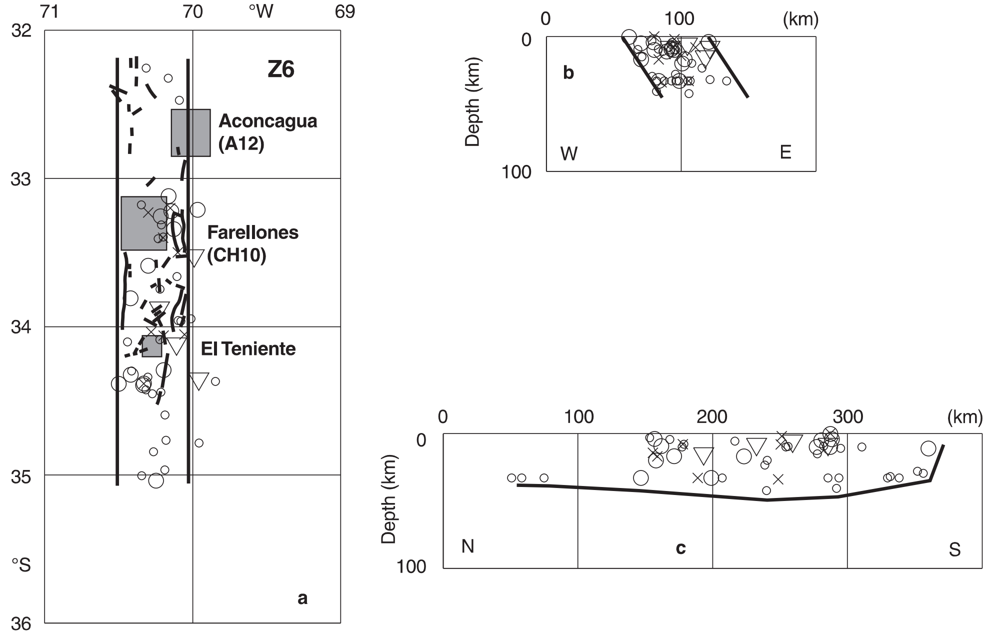

Fig. 8a–c Location of the Farellones fracture zone *Z6* with associated earthquakes **a**, transverse section **b** across and longitudinal section **c** along the fracture zone. For key see Fig. 4

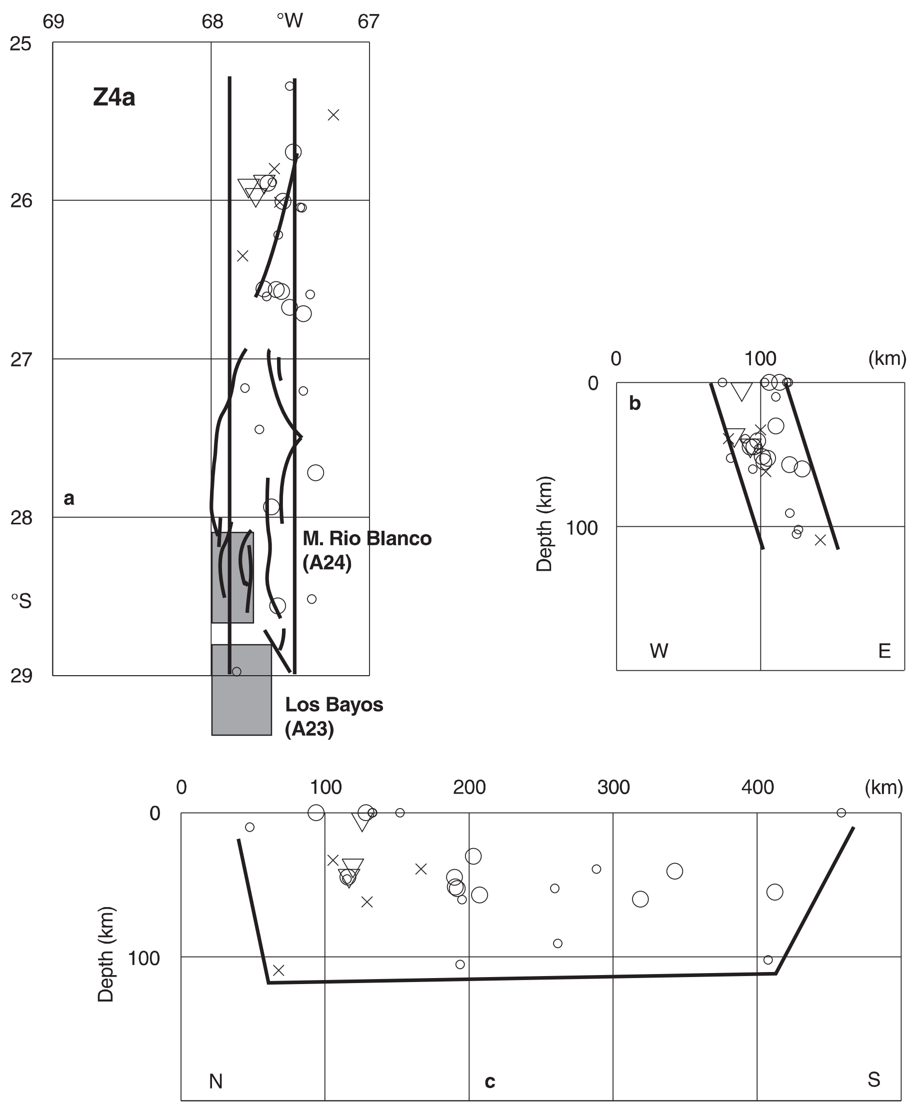

Fig. 9a–c Location of the Río Blanco-Los Bayos fracture zone *Z4a* with associated earthquakes **a**, transverse section **b** across and longitudinal section **c** along the fracture zone. For key see Fig. 4

Table 2 Co-ordination of dated deposits to individual fracture zones in periods A–D

Period	Fracture zone	Deposit				
		District	Name	Type	Age [Ma]	Reference
A 13–4 Ma	Choquelimpie Z2a	CH1	Choquelimpie	Epithermal Ag-Au-Pb-Zn	6.6	G91
	Maricunga Y6 eastern part	A18	Bajo del Durazno Bajo de Pampitas Bajo de San Lucas Mi Vida	Porphyry copper	7.9–6.8	S77, S81
	Río Blanco – Los Bayos	A23	Los Bayos	Porphyry copper	5.7	S81
	Z4a southern part	A24	Several deposits	Porphyry copper – gold	8	S97
	Carachas-Portillo Z1 northern part	A6	Chita	W-bearing porphyry copper	11.7	S77, S81
	Farellones Z6	CH11	Los Pelambres	Porphyry copper	9.8	S77
		A25	Cerro Mercedario	Porphyry copper	13	S77, S81
		A12	Río de las Vacas	Porphyry copper	8.5	S77, S81
		CH10	Bronses del Río Blanco	Porphyry copper	5–4	S91
	South of 34°S	–	El Teniente	Porphyry copper	5.6–4.3	S81
	Northern prolongation	CH14	El Indio	Au-Ag-Cu veins	13–8	S91
					11–9	DM91
B 23–12 Ma	Tumbaya Y11	A17	Pancho Arías	Porphyry copper	15.4	S77, S81
	Incahuasi-León Muerto Y12	A20	Inea Viejo	Porphyry copper	15	S77, S81
	Maricunga Y6 western part	CH9	Marte	Porphyry gold	14–13	V91, VS91
					12	DM91
			Lobo	Porphyry gold	13	VS91
			La Pepa	Porphyry gold	23–22	S91, VS91
			Refugio	Porphyry gold	23	S91, VS91
					22	DM91
	Carachas-Portillo Z1 southern part	A9	Paramillos Norte	Porphyry copper	16	S77, S81
C 44–28 Ma	Domeyko Z2c	CH3	Quebrada Blanca	Porphyry copper	38–36	DM91, S91
			Copaquire	Mo	37–34	DM91
		CH4	El Abra	Porphyry copper	38–37	S91
					36–34	SM96
					34–33	DM91
		CH5	Chuquicamata	Porphyry copper	36–31	SM96
					35–28	DM91
		CH6	Centinela	Porphyry copper	44	DM91
		CH7	La Escondida	Porphyry copper	35–31	SM96
					34–31	DM91
	El Salvador Y5	CH8	El Salvador	Porphyry copper	43–31	SM96
					42–39	DM91
			Potrerillos	Porphyry copper	35	SM96
					38–34	DM91
			El Hueso	Epithermal gold	38–37	DM91
D 64–49 Ma	Iquique Z2b	CH16	Cerro Colorado	Porphyry copper	58	S91
	Domeyko Z2c westwards	CH12	Faride	Epithermal Ag-Au	64–60	S91
					64	DM91
			Catalina	Cu, Mo	64–63	SM96
		CH15	Lomas Bayas	Porphyry copper	61	DM91
			Fortuna	Porphyry copper	64	DM91
	Tumbaya Y11 western prolongation	CH13	El Guanaco	Epithermal Au-Cu-Ag	49	S91
			Cachinal de la Sierra	Epithermal Ag-Au	59–56	DM91

DM91: Davidson and Mpodozis 1991; G91: Gröpper et al. 1991; S77: Sillitoe 1977; S81: Silitoe 1981; S91: Sillitoe 1991; S97: Sillitoe 1997; SM96: Sillitoe and McKee 1996; V91: Vila et al. 1991; VS91: Vila and Sillitoe 1991

mum depth of earthquakes of 600–650 km, corresponds to a length of about 1000 km for the subduction zone, the duration of one completed subduction cycle would be about 17 Ma at the subduction rate of 6 cm/y. On the basis of these suppositions, the following model of the history of subduction cycles in the region considered may be constructed: subduction cycle (a): 12–0 Ma, subduction cycle (b): 29–12 Ma, subduction cycle (c): 46–29 Ma, subduction cycle (d): 63–46 Ma.

If we compare the history of subduction (a–d) with the periods (A–D) of hypogene metallogeny, we see that

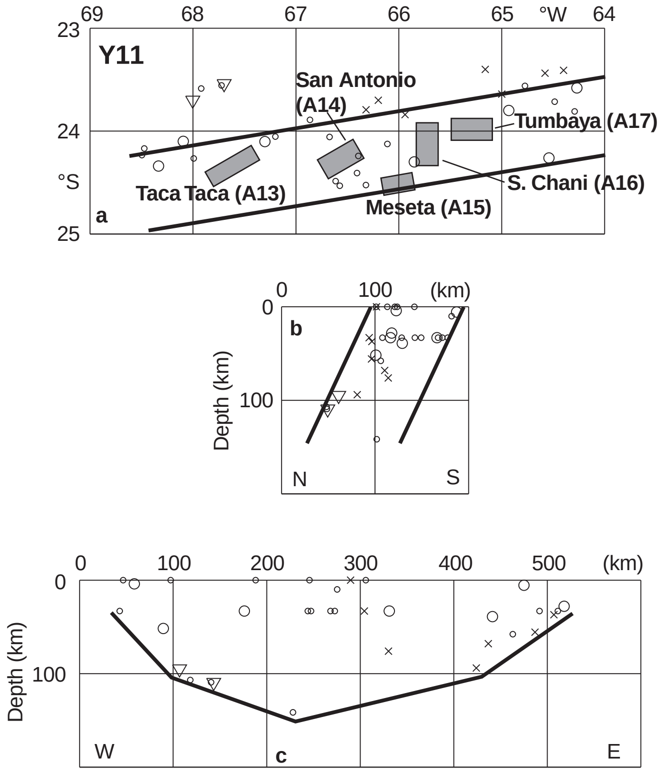

Fig. 10a–c Location of the Tumbaya fracture zone *Y11* with associated earthquakes **a**, transverse section **b** across and longitudinal section **c** along the fracture zone. For key see Fig. 4

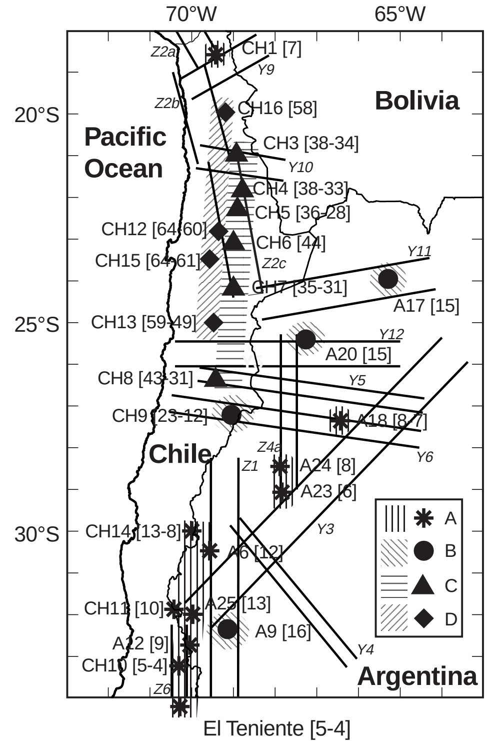

Fig. 11 Distribution of metallogenic belts and mineral deposits of different age in the framework of the seismically active fracture zones. Ages in Ma are given at individual mining districts in *brackets*; *A*: Upper Miocene-Pliocene, *B*: Upper Oligocene-Middle Miocene, *C*: Upper Eocene-Middle Oligocene, *D*: Lower Paleocene-Upper Eocene

this very simplified scheme agrees surprisingly well with the cyclic metallogenic development of the region based on radiometric dating. It should be noted that this model of the history of subduction of the Pacific floor beneath the South American plate is subject to a number of unprovable suppositions as, e.g., length of paleosubduction zones, time of the South Farallon plate break-up and subduction rates due to Cenozoic plate motions (Minster and Jordan 1978, Gordon and Jurdy 1986).

It seems that the active fracture zones, penetrating the whole thickness of the continental lithosphere, effect a channelling of ore-bearing solutions. The repeated seismic activity also seems to assure the long-term permanent re-opening of the import paths for ore-bearing solutions and thus makes it possible to accumulate enormous amounts of metals in relatively restricted domains of the Earth's crust.

A similar structural control of the distribution of calc-alkaline volcanism due to the existence of seismically active fracture zones was observed in several convergent plate margins (Hanuš and Vaněk 1984, 1985, 1987). The preferential intrusion of volcanic bodies into the framework of the fracture zones in the continental wedges, which are permanently activated and tectonically fractured by the cyclic process of subduction, may be presumed to represent one of the most important factors facilitating the formation of deposits of porphyry copper type. The ability of intrusive bodies to undergo brittle fracturing leads to the permanent production of open spaces for the penetration of hydrothermal solutions and for long-term successive deposition of ore minerals.

This model suggests the first approach to the problem of the formation of large accumulations of metals at convergent plate margins in relation to the active tectonic pattern of the continental wedges above subduction zones shown by the seismically active fracture zones in the continental lithophere. However, it must be stated that the problem is more complex because the formation of mineral deposits now exposed at the earth's surface in the continental wedge need not be directly related to the recent process of subduction because these deposits could be created by earlier cycles of subduction. The uplifting of the continental wedge, accompanying the initial stage of each subduction cycle, seems to be an essential factor for the emplacement of subduction-related mineral deposits into the mineable levels of the Earth's crust. The occurrence of mineral deposits in recently active fracture zones also seems to indicate that these fracture zones displayed activity during the earlier-cycles of subduction, prior to the uplifting of their mineralized levels into the recent near-surface position.

Acknowledgements The present work has been performed within the framework of IGCP projects 345 "Andean Lithospheric Evolution'' and 354 ''Economic Super-accumulations of Metals in the Lithosphere''. Financial support by the Grant Agency of the Czech Republic under Grant 205/95/0264 and by the Grant Agency of the Academy of Sciences of the Czech Republic under Grant A 3012805 is acknowledged. The manuscript was substantially modified and improved after the reviews of Mineralium Deposita referees (John Grocott and one anonymous referee) and valuable suggestions of the editor David Rickard and associate editor Lluis Fonboté. The authors wish to thank Jan Kutina for his assistence in obtaining map materials and for many stimulating discussions. One of the authors (V.H.) is indebted to the staff of the Departamento de Geología de la Universidad de Chile in Santiago for the possibility of visiting several Chilean mineral deposits during his OAS mission in Chile.

References

Cahill T, Isacks BL (1992) Seismicity and shape of the subducted Nazca plate. J Geophys Res 97: 17503–17529

Camus F, Skewes MA (1991) The Faride epithermal silver-gold deposit, Antofagasta region. Chile. Econ Geol 86: 1222–1237

Corvalan J (ed) (1981) Plate-tectonic Map of the Circum-Pacific Region, southeast quadrant. Am Assoc Pet Geol

Davidson J, Mpodozis C (1991) Regional geological setting of epithermal gold deposits. Chile. Econ Geol 86: 1174–1186

Delouis B, Cisternas A, Dorbath L, Rivera L, Kausel E (1996) The Andean subduction one between 22 and 25°S (northern Chile): precise geometry and state of stress. Tectonophysics 59: 81–100

Dewey JF, Lamb SH (1992) Active tectonics of the Andes. Tectonophysics 205: 79–95

Ericksen GE, Eyzaguirre VR, Urquidi BF, Salas OR (1986) Neogene-Quaternary volcanism and mineralization in the Central Andes. Trans Fourth Circum-Pacific Energy and Mineral Resources Conf. Singapore, pp 537–550

Fletcher CJN, Hawkins MP, Tejada R (1989) Structural control and genesis of polymetallic deposits in the Altiplano and Western Cordillera of southern Peru. J South Am Earth Sci 2: 61–71

Francis PW, Halls C, Baker MCW (1983) Relationships between mineralization and silicic volcanism in the Central Andes. J Volcanol Geothermal Res 18: 165–190

Frutos J (1982) Andean metallogeny related to the tectonic and petrologic evolution of the Cordillera. Some remarkable points. In: Amstutz GC, et al. (eds) Ore genesis, The state of the art. Springer. Berlin Heidelberg New York, pp 493–507

Gordon RG, Jurdy DM (1986) Cenozoic global plate motions. J Geophys Res 91: 12389–12406

Gröpper H, Calvo M, Crespo H, Bisso CR, Cuadra WA, Dunkerley PM, Aguirre E (1991) The epithermal gold-silver deposit of Choquelimpie, Northern Chile. Econ Geol 86: 1206–1221

Gustafson LB, Quiroga GJ (1995) Patterns of mineralization and alteration below the porphyry copper orebody at El Salvador, Chile. Econ Geol 90: 2–16

Hanuš V, Vaněk J (1976) Intermediate aseismicity of the Andean subduction zone and recent andesitic volcanism. J Geophys 42: 219–223

Hanuš V, Vaněk J (1977–78) Subduction of the Cocos plate and deep fracture zones of Mexico. Geofís Int 17: 14–53

Hanuš V, Vaněk J (1978) Morphology of the Andean Wadati-Benioff zone, andesitic volcanism, and tectonic features of the Nazca plate. Tectonophysics 44: 65–77

Hanuš V, Vaněk J (1983) Deep structure of the Vanuatu (New Hebrides) island arc: intermediate depth collision of subducted lithospheric plates. NZJ Geol Geophys 26: 133–154

Hanuš V, Vaněk J (1984) Earthquake distribution and volcanism in Kamchatka, Kurile Islands, and Hokkaido. Studia Geophys Geod 28: 36–55, 129–148, 248–271

Hanuš V, Vaněk J (1985) Structure of Wadati-Benioff zones and volcanism produced by the process of subduction. Tectonophysics 112: 51–67

Hanuš V, Vaněk J (1987) Deep seismically active fracture zones in Ecuador and northern Peru. Studia Geophys Geod 31: 8–25, 156–175

Hanuš V, Vaněk J (1991) Paleoplates buried in the upper mantle and the cyclic character of subduction. J Geodynamics 13: 29–45

Hanuš V, Vaněk J (1992) Seismotectonics of continental wedges overlying circum-Pacific subduction zones. Cas Min Geol (Prague) 37: 277–287

Hanuš V, Vaněk J (1996) Cyclic evolution of convergent plate margins indicated by time sequence of volcanism and subduction. Global Tectonics and Metallogeny 5: 103–108

Hanuš V, Vaněk J, Špičák A (1996) Seismically active fracture zones in the continental wedge of the central part of Andean South America. Géodynamique andine, ORSTOM editions, Colloques et séminaires, Paris, pp 187–190

Jannas RR, Beane RE, Ahler BA, Brosnahan DR (1990) Gold and copper mineralization at the E1 Indio deposit, Chile. J Geochem Exploration 36: 233–266

Mapa Geológico de Chile (1:1 000 000), 1982. Servicio Nacional de Geologia y Minería, Santiago

Mapa Geológico de la República Argentina (1:2 500 000), 1982. Servicio Geológico Nacional, Buenos Aires

Mapa Minero (1:750 000). Provincias de San Juan, Mendoza, Salta y Jujuy, 1966. Instituto Nacional de Geología y Minería, Buenos Aires

Marschik R, Singer BS, Munizaga F, Tassinari C, Moritz R, Fontboté L (1997) Age of Cu (-Fe) – Au mineralization and thermal evolution of the Punta del Cobre district, Chile. Miner Deposita 32: 531–546

Mc Kee EH, Robinson AC, Rybuta JJ, Cuitinno L, Moscoso RD (1994) Age and Sr isotopic composition of volcanic rocks in the Maricunga Belt, Chile: implications for magma sources. J South Am Earth Sci 7: 167–177

Minster JB, Jordan TH (1978) Present-day plate motions. J Geophys Res 83: 5331–5354

Mitchell AHG (1973) Metallogenic belts and angle of dip of Benioff zones. Nature 245: 49–52

Mitchell AHG, Beckinsale RD (1982) Mineral deposits associated with calc-alkaline rocks. In: Thorpe RS (ed). Andesites. Wiley, New York, pp 677–695

Regional Catalogue of Earthquakes (1964–1993) International Seismological Centre, Edinburgh and Newbury

Sillitoe RH (1972) A plate tectonic model for the origin of porphyry copper deposits. Econ Geol 67: 184–197

Sillitoe RH (1974) Tectonic segmentation of the Andes: implications for magmatism and metallogeny. Nature 250: 542–545

Sillitoe RH (1976) Andean mineralization: a model for the metallogeny of convergent plate margins. In: Strong DF (ed) Metallogeny and plate tectonics. Geol Assoc Can Spec Pap 14: 59–100

Sillitoe RH (1977) Perino-Carboniferous, Upper Cretaceous, and Miocene porphyry copper-type mineralization in the Argentinian Andes. Econ Geol 72: 99–103

Sillitoe RH (1981) Regional aspects of the Andean porphyry copper belt in Chile and Argentina. Transactions, Institution of Mining and Metallurgy, Section B 90: B15–B36

Sillitoe RH (1988) Epochs of intrusion-related copper mineralization in the Andes. J South Am Earth Sci 1: 89–107

Sillitoe RH (1991) Gold metallogeny of Chile – an introduction. Econ Geol 86: 1187–1205

Sillitoe RH (1992) Gold and copper metallogeny of the Central Andes – past, present, and future exploration objectives. Econ Geol 87: 2205–2216

Sillitoe RH (1997) Characteristics and controls of the largest porphyry copper-gold and epithermal gold deposits in the circum-Pacific region. Australian J Earth Sci 44: 373–388

Sillitoe RH, McKee EH (1996) Age of supergene oxidation and enrichment in the Chilean porphyry copper province. Econ Geol 91: 164–179

Sillitoe RH, McKee EH, Vila T (1991) Reconnaissance K-Ar geochronology of the Maricunga gold-silver belt, Northern Chile. Econ Geol 86: 1261–1270

Skewes MA, Stern CR (1994) Tectonic trigger for the formation of late Miocene Curich breccia pipes in the Andes of central Chile. Geology 22: 551–554

Soler P, Bonhomme MG (1988) New K-Ar age determinations of intrusive rocks from the Cordillera Occidental and Altiplano of central Peru: Identification of magmatic pulses and episodes of mineralization. J South Am Earth Sci 1: 169–177

Ulriksen G (1990) Mapa Metalogénico de Chile entre los 18° and 34°S (1:1 000 000) Servicio Nacional de Geologia y Minas – Chile. Santiago. Boletín No. 42: 1–112

Vaněk J, Hanuš V, Slancová A, Špičák A (1999) Seismically active fracture zones in the continental wedge above the subduction zone in the Arica Elbow region. Studia Geophys Geod 43 (in press)

Vila T, Sillitoe RH (1991) Gold-rich porphyry systems in the Maricunga belt, Northern Chile. Econ Geol 86: 1238–1260

Vila T, Sillitoe RH, Betzhold J, Viteri E (1991) The porphyry gold deposit at Marte, Northern Chile. Econ Geol 86: 1271–1286